

## 24.3: Optical and Mechanical Properties of Stretched PDLC Films for Scattering Polarizers

Ichiro Amimori<sup>†</sup>, James N. Eakin, Gregory P. Crawford

Division of Engineering, Brown University, Providence, RI, USA

Nikolai V. Priezjev, Robert A. Pelcovits

Department of Physics, Brown University, Providence, RI, USA

### Abstract

By stretching (tensile strain) a polymer dispersed liquid crystal (PDLC) film the liquid crystal droplets become elliptical and a polarization separation optical element is created. These films have significant potential as scattering polarizers in liquid crystal displays (LCDs). We present a relationship between the polarization properties and the tensile strain properties of PDLC scattering polarizers. In addition, we present a modeling approach using a Monte-Carlo technique to predict the alignment of liquid crystals within the droplets and the details of their surface anchoring at the cavity wall. We also extend our investigation to reactive mesogen liquid crystal and higher order liquid crystal phases, such as ferroelectric and smectic A liquid crystal materials.

### 1. Introduction

Power consumption of a LCD is of the utmost importance for portable applications. In typical high resolution LCDs utilized in laptop computer applications, the optical efficiency is approximately 6%. One of the primary reasons for energy loss is

the absorbing polarizers. Conventional polarizers based on absorption are iodine doped polyvinyl alcohol films that absorb >50% of the incident light (see Figure 1(a)).

It has been reported that a stretched PDLC film has a polarization selectivity that arises from anisotropic scattering of aligned liquid crystal droplets in a polymer matrix as shown in Figure 1(b) [1]. By utilizing these films for LCD applications, scattered light can be recycled in a backlight system to ultimately improve the optical efficiency [2]. From a technology perspective scattering polarizers need to be inexpensive and simple to fabricate to realize their potential use in commercial applications. Analogous approaches to scattering polarizers incorporate optically isotropic glass beads in stretched polymer films [3].

We report a comprehensive study on the basic properties of PDLC scattering polarizers, including the delicate relationship between polarization selectivity and tensile strain during fabrication, and we also develop a model based on Monte-Carlo simulation to understand the details of the liquid crystal director configuration and the underlying physical principles that govern the aligned configuration.

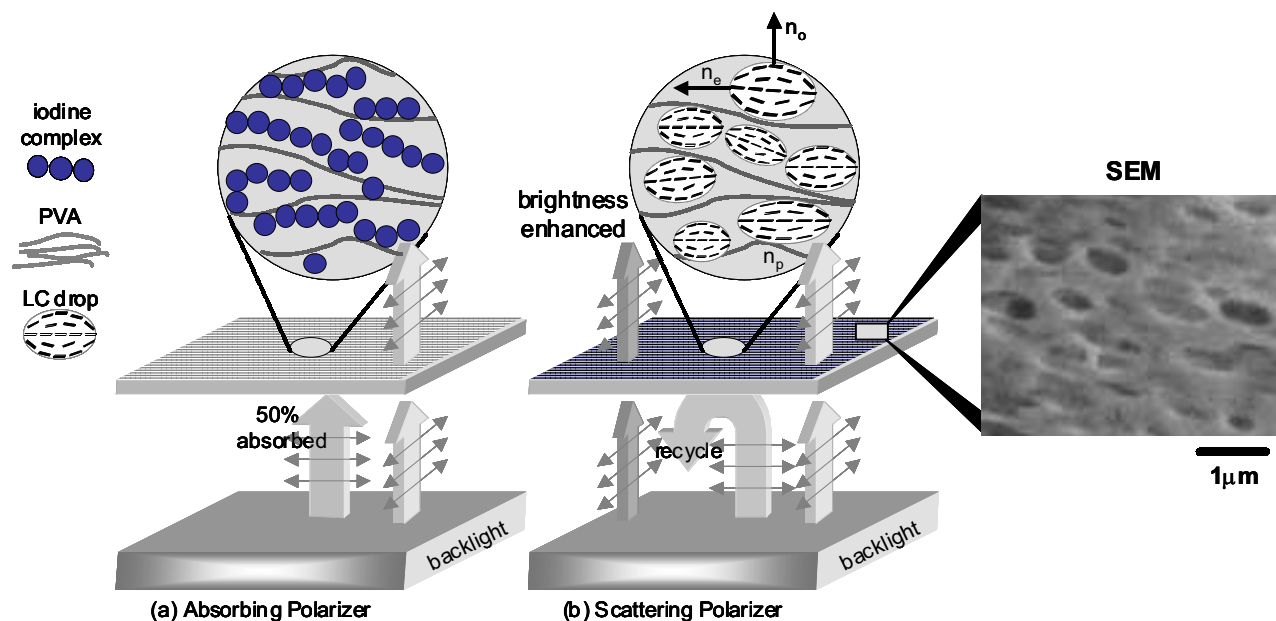


Figure 1 A conventional absorbing polarizer is presented in (a) and a scattering polarizer based on PDLC technology is presented in (b). In (b), the refractive index of polymer,  $n_p$ , matches that of the ordinary refractive index,  $n_o$ , of the liquid crystal.

## 2. Experiment and Results

### 2-1. PDLC Film samples

Polymer dispersed liquid crystal (PDLC) films used in this contribution consist of dispersions of liquid crystals and polyvinyl alcohol (PVA), which is a water-soluble polymer. A 20 wt% aqueous solution of PVA is mixed with the liquid crystal E7 and then dispersed in water [4]. We used an ultrasonic probe to emulsify the liquid crystal into the PVA aqueous solution. The emulsion was coated on a smooth polyethylene terephthalate (PET) substrate using a Meyer Bar and dried under ambient conditions. The film was then peeled from the substrate. The film thickness was approximately 12  $\mu\text{m}$  and the concentration of liquid crystal in the film is 25 wt%. The PDLC films were unidirectionally stretched by a tensile tester (MINIMAT2000) with the draw rate of 0.1 mm/min.

### 2-2. The Optics of Stretched PDLC Films

Figure 2 demonstrates the shape of droplets after stretching. The director configuration in the droplets aligns parallel to the tensile strain direction thereby creating a refractive index difference between axes parallel and perpendicular to the tensile axis. The refractive index of PVA is almost isotropic since its birefringence is relatively small. As a result, a large refractive index mismatch exists in a direction parallel to the tensile axis and a match occurs in a direction perpendicular to the tensile axis because the ordinary refractive index  $n_o$  of the liquid crystal is approximately that of the polymer,  $n_p$  as shown in Figure 3. The aspect ratio of the stretched droplet shown in Figure 2(b) is approximately 4:1 for 100% strain since the width also shrinks while stretching. This optical structure creates an anisotropic scattering condition.

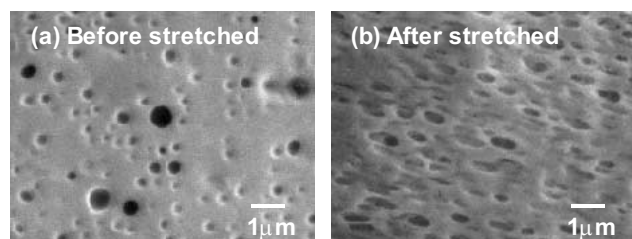


Figure 2 The SEM pictures of E7/PVA PDLC films before (a) and after stretching (b). The strain in (b) was 100%.

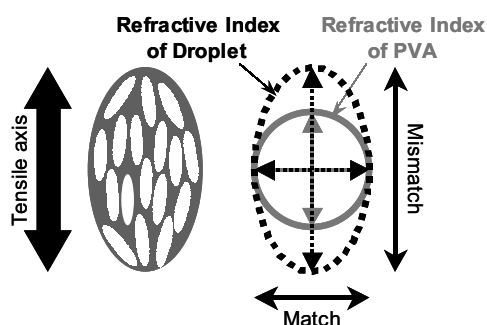


Figure 3 The distinction in refractive indices between liquid crystal droplets and PVA in stretched PDLC films.

### 2-3. Mechanical and Optical Properties of Stretched PDLC films

The stress strain curve in Figure 4(a) and 4(b) show the transmittances of two polarizations, parallel ( $T_{\parallel}$ ) and perpendicular ( $T_{\perp}$ ) to the tensile axis. Figure 4(a) shows the strain range from 0% to 100% and Figure 4(b) shows the expanded view with the strain range from 0 to 30%.

As the strain increases,  $T_{\perp}$  increases and  $T_{\parallel}$  decreases. This reflects the change in the liquid crystal alignment along the tensile axis. The stress-strain curve is linear to the maximum value (elastic region) and then begins to decrease. The polarization selectivity appears strongly only after the elastic region is reached, as shown on the stress-strain curve in Figure 4(b). It can be considered that the stress decay in region 2 corresponds to polymer chain alignment that relaxes the stress within the film [5]. Also this result suggests that the polymer orientation also contributes to the liquid crystal alignment within the droplet as well as the shape anisotropy of the droplet because of the large dependence on strain in region 2. In the elastic regime, there is very little separation  $T_{\parallel}$  and  $T_{\perp}$  as shown in Figure 4(b).

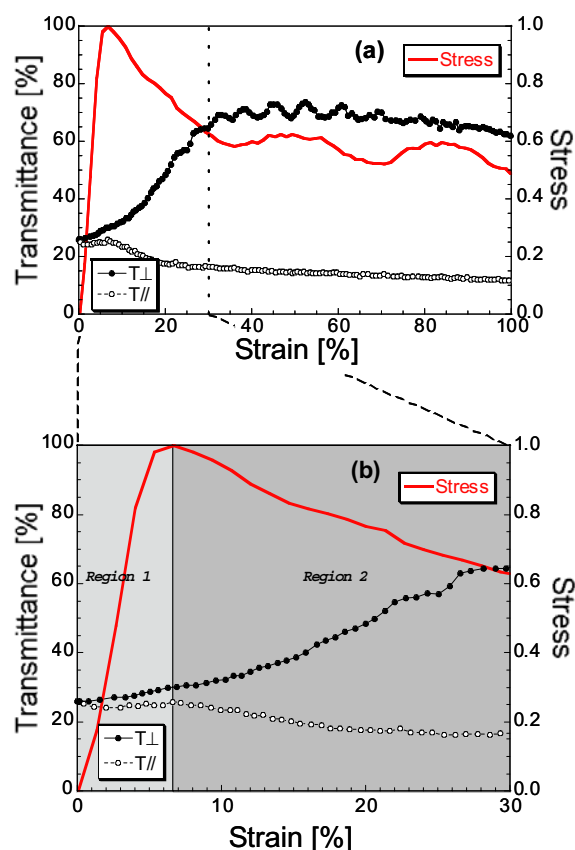


Figure 4 The stress strain curve (line) and the polarization selectivity (data points) of light polarized parallel  $T_{\parallel}$  and perpendicular  $T_{\perp}$  to the tensile axis (left). An expanded view of the elastic region (region 1) can be seen in (b).

### 3. Monte-Carlo Simulations for PDLC

#### 3-1. Lebwohl-Lasher Model for PDLC.

We also report the results of Monte-Carlo simulations of the Lebwohl-Lasher lattice model of liquid crystals confined to spherical and elliptical cavities with homogeneous boundary conditions [6]. Although we cannot separate out the effects of shape anisotropy and alignment due to the polymer chains in the matrix at this time, these effects can be accounted for in the model. This model represents each mesogenic molecule by a three-dimensional spin vector. These molecules are free to rotate about their centers, which are fixed on the lattice sites.

The bulk Lebwohl-Lasher pair potential is described as  $U_{ij} = -\epsilon_b P_2(\cos\theta_{ij})$  where  $\theta_{ij}$  is the angle between two molecules  $i$  and  $j$ ,  $P_2$  is a second rank Legendre polynomial, and  $\epsilon_b$  is a positive constant for nearest-neighbor sites and zero otherwise.

The homogeneous surface anchoring is introduced via a group of boundary layer molecules located on the outside surface of the droplet wall. The interaction of these molecules with those inside the droplet wall is described by the potential  $U_{ik} = -\epsilon_s P_2(\cos\theta_{ik})$  where spin  $i$  is located inside the boundary and spin  $k$  is the nearest-neighbor spin that belongs to the boundary layer. The constant  $\epsilon_s$  is the surface anchoring strength. The total potential energy in a droplet is given by the sum of these potentials over all pairs of molecules.

#### 3-2. LC Alignment in PDLC Droplets

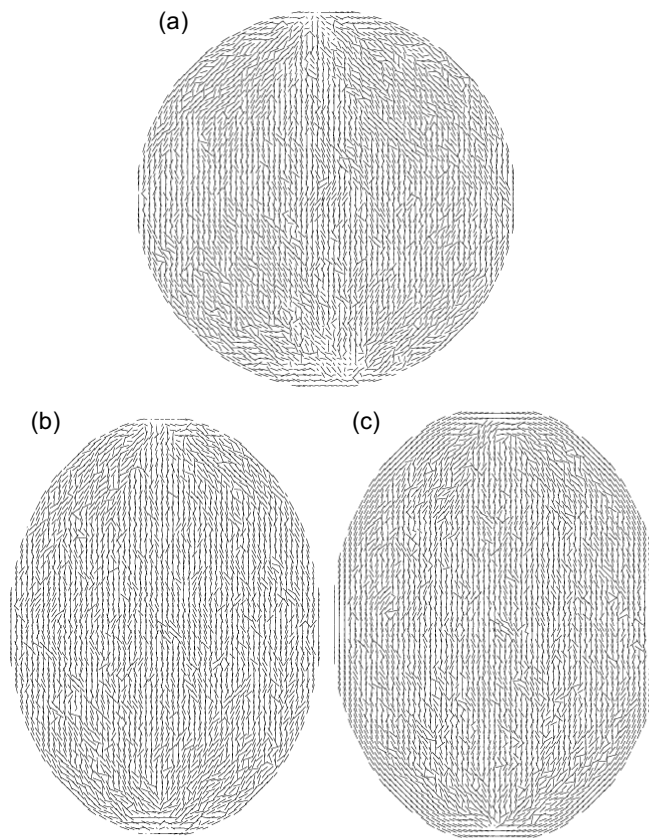
##### 3-2-1. Comparison of spherical and elliptical droplets in the absence of polymer alignment

Figure 5 shows the liquid crystalline ordering for spherical and elliptical droplets simulated with the Lebwohl-Lasher model described above, in the absence of the surface anchoring potential proportional to  $\epsilon_s$ . The molecules at the droplet wall are confined to the local tangential plane, but are otherwise free to rotate. In both cases, an ordered bipolar structure was formed. For the spherical droplet the direction of the nematic director is not predetermined; by symmetry the alignment can occur along any diameter of the sphere. On the other hand, for the elliptical droplet the director always aligns with the long axis of the droplet.

##### 3-2-2. Effect of polymer alignment

The experimental measurements described in Section 2 indicate that the polymer alignment influences the liquid crystalline order. To study this effect we simulated the Lebwohl-Lasher model including the surface anchoring potential. The molecules in the boundary layer are now assumed to be oriented permanently along the meridians of the ellipsoid, to mimic the interaction with the ordered polymer strands.

Figure 5(b) and (c) compares the liquid crystalline order with and without polymer alignment. The difference is not significant pictorially but we find that the average nematic order parameter in the presence of polymer alignment is 0.63, compared to 0.60 in the absence of alignment. These results are consistent with the results of the mechanical and optical experiments.



**Figure 5** Liquid crystal alignment in PDLC droplets simulated by the Lebwohl-Lasher model: (a) Spherical without polymer alignment; (b) Elliptical without polymer alignment; and (c) Elliptical with polymer alignment.

### 4. Applications

#### 4-1. Application for Polarizers

In order to utilize PDLC scattering polarizers in LCD applications, high polarizing efficiency is a prerequisite. Polarizing efficiency,  $\eta_p$ , is defined by the following equation.

$$\eta_p = \sqrt{\frac{T_{\perp} - T_{\parallel}}{T_{\perp} + T_{\parallel}}} \quad [1]$$

where,  $T_{\perp}$  is a transmittance of transmission axis and  $T_{\parallel}$  is the scattering axis [7].

Figure 6 shows the dependence of  $T_{\perp}$ ,  $T_{\parallel}$  and polarizing efficiencies on film thickness. Strain was 100% and thickness was controlled by stacking same films. By increasing the thickness of the PDLC, the polarizing efficiency can be enhanced as shown in Figure 6.

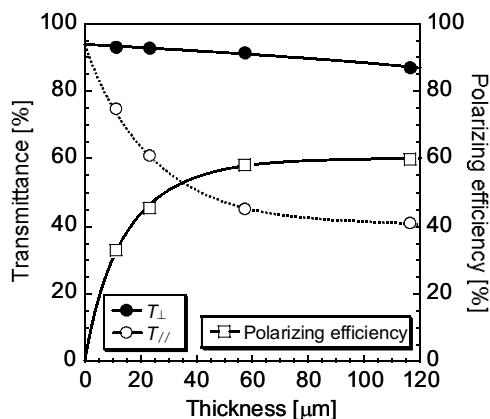


Figure 6 The dependence of  $T_{\perp}$ ,  $T_{\parallel}$  and polarizing efficiencies on film thickness. A white light illumination source and integrating sphere were used in this measurement.

## 5. Other Materials

Using reactive mesogen liquid crystals and curing the shaped droplets in UV light allows us to capture the liquid crystal alignment and the shape anisotropy indefinitely.

Figure 7 shows SEM pictures of solid elliptical droplets created from LC242 (BASF). After PDLC films were fabricated, stretched, and photopolymerized, the PVA was dissolved with water and the particles were separated out.

Figure 8 shows the dependence of polarizing efficiency on temperature. The differences in the measurement of  $\eta_p$  between Figure 6 and 8 depend the measurement technique. A white light source and integrating sphere were used in Figure 6, while a polarized He-Ne laser was used to generate the data in Figure 8.

Nematic, smectic A and ferroelectric liquid crystals lose their polarizing efficiency at temperatures above their isotropic transition points. Above the transition point scattering ceases since the refractive index of the liquid crystal in the isotropic phase nearly matches that of the polymer for all polarizations. The uncured reactive mesogen liquid crystals show decreasing polarizing efficiency at 125°C. However, reactive mesogen liquid crystals cured by UV show stable polarizing efficiency well over 125°C. The magnitude of the polarizing efficiency is still low because  $\Delta n$  of this particular material is small. These results suggest that PDLC scattering polarizers with reactive mesogen liquid crystals have a great potential for temperature stability.

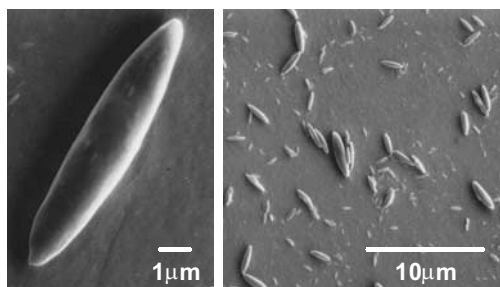


Figure 7 The SEM picture of elliptical cured liquid crystal particles obtained from stretched PDLC films.

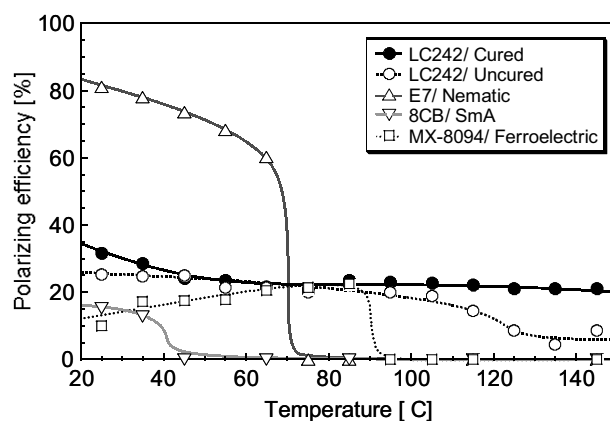


Figure 8 The dependence of polarization efficiencies on temperature using 633 nm He-Ne laser. Polarizing efficiency was calculated from transmittances without scattered light.

## 6. Summary

By simultaneously monitoring the stress-strain characteristics and the transmittance parallel and perpendicular to the tensile axis of stretch PDLC films, we have presented the relationship between the polarization properties and tensile strain properties of PDLC scattering polarizers. We have predicted the details of nematic liquid crystal director configuration in the framework of a Monte Carlo model where both shape anisotropy and the subtle details of surface anchoring can be accounted for. We have extended our work to include higher order liquid crystal phases in this application, and have demonstrated a virtually temperature independent scattering polarizers by aligning a reactive mesogen material.

## 7. Acknowledgement

R.A.P. gratefully acknowledge the support of the National Science Foundation (DMR98-73849), and G.P.C. wishes to thank the NSF/MRSEC Center (DMR-0079964) and his NSF Career Grant (DMR-9875427).

## 8. References

- [1] O. A. Aphonin, YU. V. Panina, A. B. Pradin and D. A. Yakolev: *Liq. Cryst.*, **15**, 395 (1993).
- [2] E. Lueder: *Liquid Crystal Displays* (John Wiley & Sons, Chichester 2001).
- [3] H. Jagt, Y. Dirix, R. Hikmet and C. Bastiaansen: *Jpn. J. Appl. Phys. Part 1*, **37**, 4389 (1998).
- [4] P. S. Drzaic: *J. Appl. Phys.*, **60**, 2142 (1986).
- [5] L. H. Sperling: *Introduction to Physical Polymer Science*. 2<sup>nd</sup> Edition (John Wiley & Sons, NY 1992).
- [6] N. V. Priezjev and R. A. Pelcovits: *Phys. Rev. E*, **62**, 6734 (2000).
- [7] R. Mizoguchi, K. Kobayashi, T. Shimomura and S. Kobayashi: *Displays*, 201 (1983).